

6.1.5 Effect of processing temperature on the Ag diffusion

In this section we will investigate the relevance of T_{max} i.e., the maximum temperature used during the welding process. It is a temperature between the peritectic temperature of the YBCO material ($T_p \simeq 1010^\circ\text{C}$) and the melting point of YBCO/Ag composite ($T_p \simeq 970^\circ\text{C}$). At this temperature the Ag foil melts and diffuses into the YBCO matrix according to the equation 6.2 and inducing the melting of the interface according to equation 6.4. It is obvious that if Ag diffusion is a temperature activated phenomenon, this is another parameter which should be controlled in order to optimize the extension of the molten interface. Thus, investigation of this crucial parameter has been done in order to control the Ag diffusion into YBCO solid by means of slow cooling experiments. A $10\mu\text{m}$ Ag foil and a cooling rate of $0.6^\circ\text{C}/\text{h}$ was used to study the processing temperature on the Ag diffusion into previously non-oxygenated YBCO monoliths.

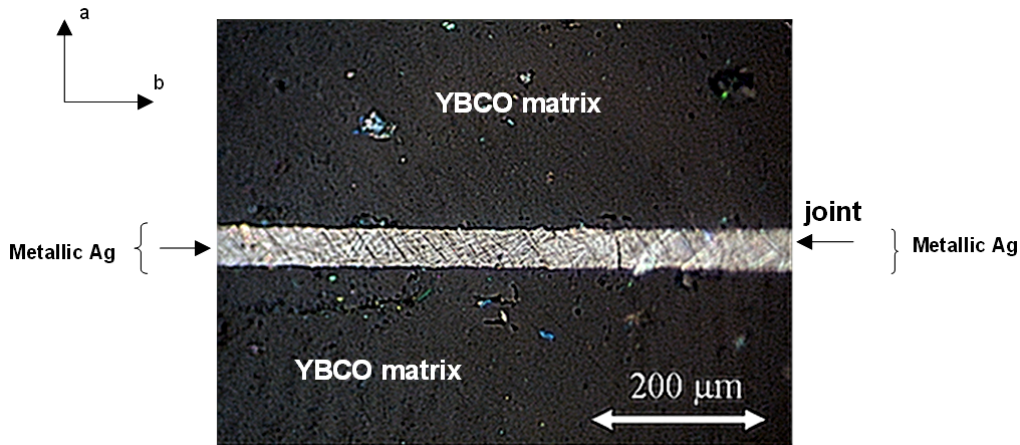


Figure 6.36: Optical micrograph of the ab plane of a joint obtained by heating it to $T_{max}=985^\circ\text{C}$ and held for. The initial thickness of the Ag foil was of $g_{Ag}=10\mu\text{m}$. The white area represents metallic Ag remained at the interface.

Three different maximum temperatures have been investigated in this section: $T_{max}=985^\circ\text{C}$, which is a temperature slightly higher than the peritectic

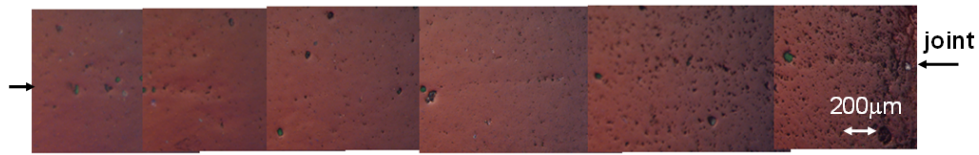
temperature of YBCO/Ag composite; $T_{max}=992^{\circ}\text{C}$ and finally a temperature $T_{max}=1005^{\circ}\text{C}$ which is a temperature close to the peritectic temperature of YBCO monolith.

Figure 6.36 shows the optical micrograph of the ab plane of the sample T_{985} . This sample was heated up to $T_{max}=985^{\circ}\text{C}$, which is a temperature higher than the melting point of the YBCO/Ag composite, and lower than the peritectic temperature of YBCO material. At this temperature the Ag foil melts but remains trapped between two YBCO blocks and the joint is not superconducting. As a consequence, we conclude that it is a temperature too low for the welding process because the diffusion of silver in the YBCO matrix is too small.

In figures 6.37 (a-b), there are represented optical micrographs showing the microstructure of both, ab (see figure 6.37a) and ac planes (see figure 6.37b) of a YBCO/Ag/YBCO interface obtained at $T_{max}=992^{\circ}\text{C}$. In both images, no Ag precipitates nor non-superconducting phases are observed at the joint area. Additionally, it can be noticed that the ac plane (figure 6.37b) displays small optically contrasted bands associated to regions with higher oxygen content which are extended at each side of the interface and sometimes crossing it. As it has been mentioned, these bands are usually generated around regions having microcracks parallel to the ab planes which then facilitate a faster oxygenation [89]. It is easy to observe that these bands are parallel at each side of the joint, thus demonstrating again the good crystallographic orientation between both YBCO pellets.

For a temperature $T_{max}=1005^{\circ}\text{C}$, just below the peritectic temperature of the YBCO material, it can be observed that the liquid is trapped at the central part of the YBCO/Ag/YBCO interface (figure 6.38). The rest of the weld has a clean and continuous microstructure. Moreover, the molten area is extended up to $500\mu\text{m}$, which indicates that this temperature is too high.

The presence of various defects, voids, pores, liquid phases and sometimes a gap between the YBCO tiles at the interface region can be noticed when the



(a)



(b)

Figure 6.37: Optical micrographs corresponding the sample T_{992} : a) ab plane; b) ac plane. The joint is indicated in the figure by white arrows.

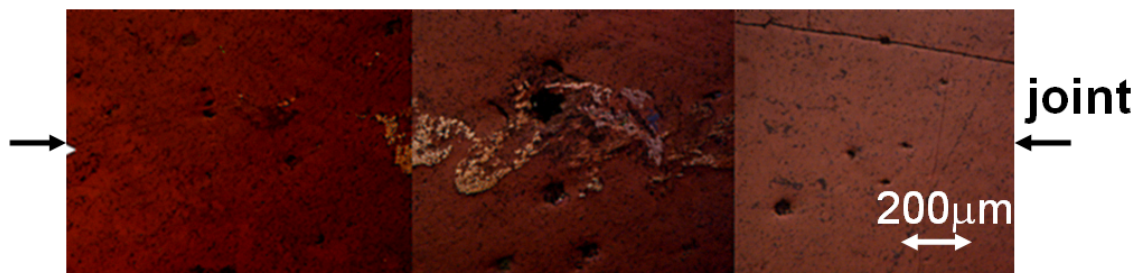


Figure 6.38: Optical micrographs showing the microstructure of the ab planes corresponding to the sample T_{1005} . The joint is indicated by arrows. The central part presents some phases which have been trapped by the interface during the welding process.

welding process is not optimized. The void/pores are basically filled with the rejected liquid phases, which are generally free of Y ions and sometimes rich in CuO phase and Ag precipitates, thus inhibiting the formation of YBCO phase in these regions. According to these results, a processing temperature T_{max} of 992°C is the best to obtain, along with the other optimized parameters, a good quality joint.

6.1.6 Effect of the temperature window on the microstructure of the final joints

In order to obtain large well-grown joints of YBCO by employing a Ag foil as spacer material, we must adjust the process time to the growth rate. The use of a "seed" allows us to act principally in a given temperature range called "window temperature". The temperature window is linked with the temperatures to which the homogeneous nucleation and the heterogeneous one take place. The highest temperature of the window is above the peritectic temperature of the YBCO/Ag composite and the lowest one below the melting point of YBCO/Ag. Thus, the heterogeneous nucleation at "the seed" takes place at a higher temperature than the homogeneous nucleation.

Thus, the assembly YBCO/Ag/YBCO is heated up to the optimized temperature $T_{max}=992^{\circ}\text{C}$ during 3 hours. Then, the sample is rapidly cooled down until the temperature where the heterogeneous nucleation occurs. The rate used to cool down the sample in the temperature window is of $0.6^{\circ}\text{C}/\text{h}$. When the lowest temperature of the window is reached, the junction is already solidified and we cool down the sample rapidly down to room temperature using a rate of $r\approx 200^{\circ}\text{C}/\text{h}$. Four different temperature windows of 18, 23, 28 and 33°C have been studied. The starting temperature of this window was 973°C , which is a temperature higher than the peritectic temperature of YBCO/Ag composites. This window, along with the cooling rate r , determines the time spent in the liquid state by the YBCO/Ag interface. The microstructure of both, ab and ac planes, of the different samples was studied by means of optical microscopy in polarized light and by scanning electron microscopy before the oxygenation step. In figures 6.39, 6.40, 6.41, 6.42 are represented the YBCO/Ag/YBCO interfaces of these samples where the joining zone is indicated by white arrows.

The first observation is that the joints grown with a small temperature window present some residual liquid phase, meaning that the liquid could not be completely solidified during the cooling time. EDX analysis of these agglomerates

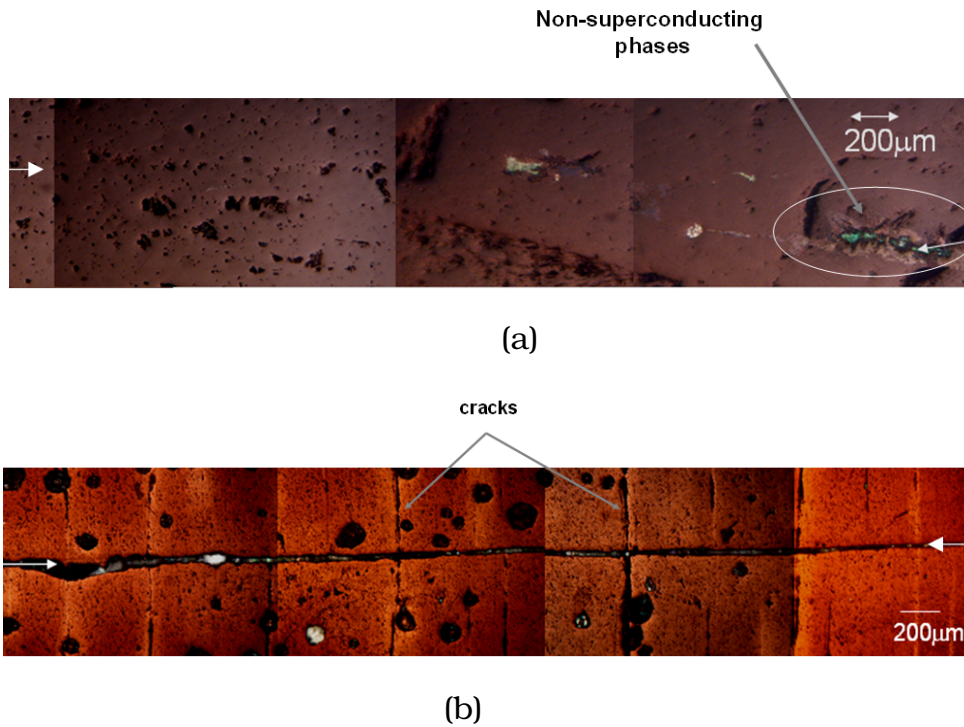


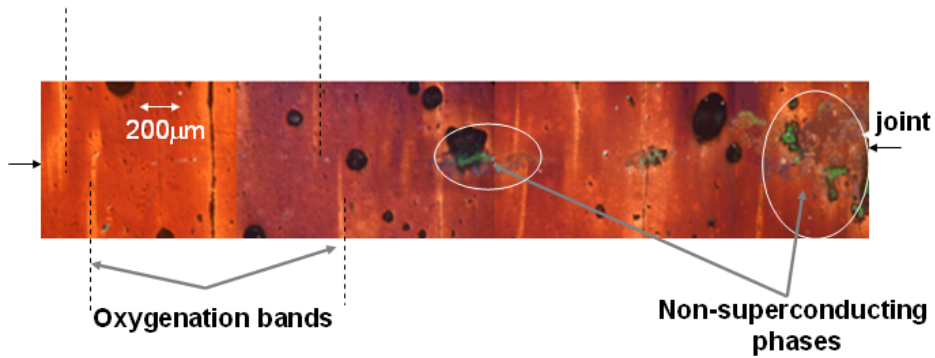
Figure 6.39: Optical micrographs corresponding the sample ΔT_{18} : a) ab plane; b) ac plane. The joints are indicated in figure by arrows.

show the existence of a mixture of Y211 particles, Ag precipitates and $BaCuO_2$ -CuO phases. Such agglomerates of non-superconducting phases at the interface between the two domains are also found in the case of the multi-seeded samples [7, 6] and they are detrimental for the supercurrent flow.

Our observations show that, enlarging the temperature window, the concentration of these phases is reduced. The complete elimination of these non-superconducting phases from the joint area occurs when the temperature windows range between 28°C and 33°C . In figure 6.42 it is represented the microstructure of ab and ac planes, respectively, of a joint obtained by cooling it down in a temperature window of 33°C . It is easy to observe that the interface is free of any non-superconducting phases (figure 6.42a). Moreover, the microcracks existing in the ac plane (figure 6.42b), are continuous across the joint indicating a crystallographic matching between both single crystals. As a conse-



(a)



(b)

Figure 6.40: Optical micrographs showing the microstructure of sample ΔT_{23} : a) ab plane; b) ac plane. The interfaces are indicated in figure by arrows.

quence, a temperature window of 28°C-33°C with a cooling rate of 0.6°C/h from $T_1=973^\circ\text{C}$ is a good choice for our samples to push away completely the Ag from the interface and to crystallize the melted zone.

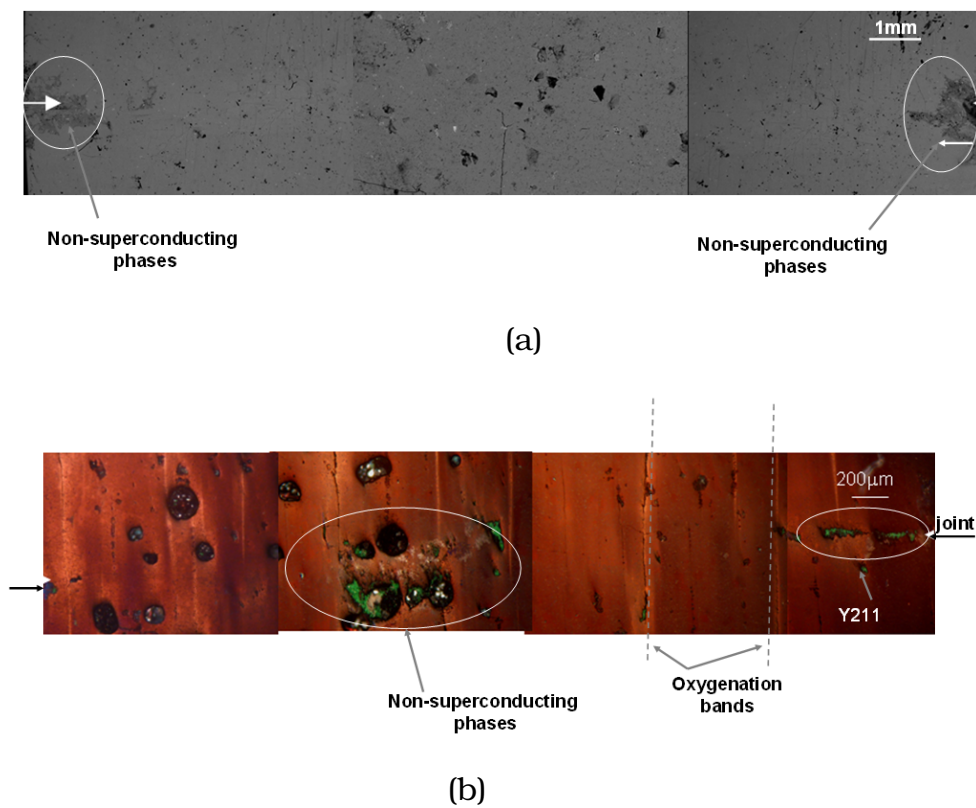
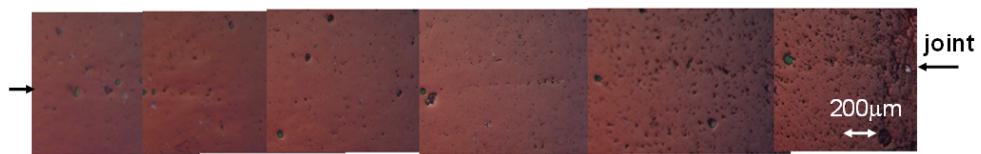
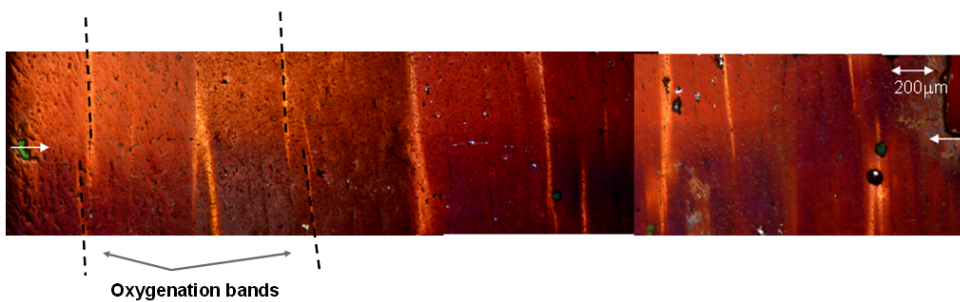


Figure 6.41: Optical micrographs showing the microstructure of the sample ΔT_{28} for: a) ab plane; b) ac plane. The interfaces are indicated in figure by arrows.



(a)



(b)

Figure 6.42: Optical micrographs showing the microstructure of the sample ΔT_{33} for: a) ab plane; b) ac plane. The interfaces are indicated in figure by arrows.

6.2 Study of the homogeneity in the microstructure of the final joints

The Ag diffusion process into YBCO material is a very complex phenomenon. In the previous sections we have analyzed the influence of different parameters into the Ag diffusion.

In this section the homogeneity of the Ag diffusion into YBCO matrix is analyzed. For this experiment, YBCO/Ag/YBCO joints have been cut in layers parallel to the ab plane so that we can study the top, the center and the bottom faces of the samples. In this way we analyze the microstructure of the joint located at 0.3cm and 0.6cm below the top face. The microstructure of each face has been analyzed by means of scanning electron microscopy and optical microscopy with polarized light. Chemical analysis on the junction have been performed by EDX.

Two samples have been used in this experiment: sample A and sample B. The sample A was obtained by following the welding process: $t_{melt}=3h$, $T_{max}=992^{\circ}C$, $r=6^{\circ}C/h$ and $\Delta T=33^{\circ}C$, whereas sample B was obtained by a welding process with the same parameters except the cooling rate which was $r=3^{\circ}C/h$. Samples A and B were characterized along the (ab)-plane to different depths, i.e. bottom, center and top face hereafter called top_A , $bottom_A$, $center_A$ and top_B , $bottom_B$, $center_B$, respectively (figure 6.43). We consider the top face being the ab plane, where the seed has been placed during the top seeding process applied in order to obtain the YBCO samples, whereas the center and bottom faces are the ab planes situated 0.3cm and 0.6cm, respectively, under the plane where the seed has been placed.

In figures 6.44 there are shown general views of the microstructure of the sample A, where figure 6.44a represents the microstructure of the top face, figure 6.44b of the center face and the figure 6.44c of the bottom face. It is interesting to observe that while moving away from the top face towards the bottom face the microstructure is changing. The first difference between the analyzed faces relates to the porosity which exhibit each face. Note that by moving away

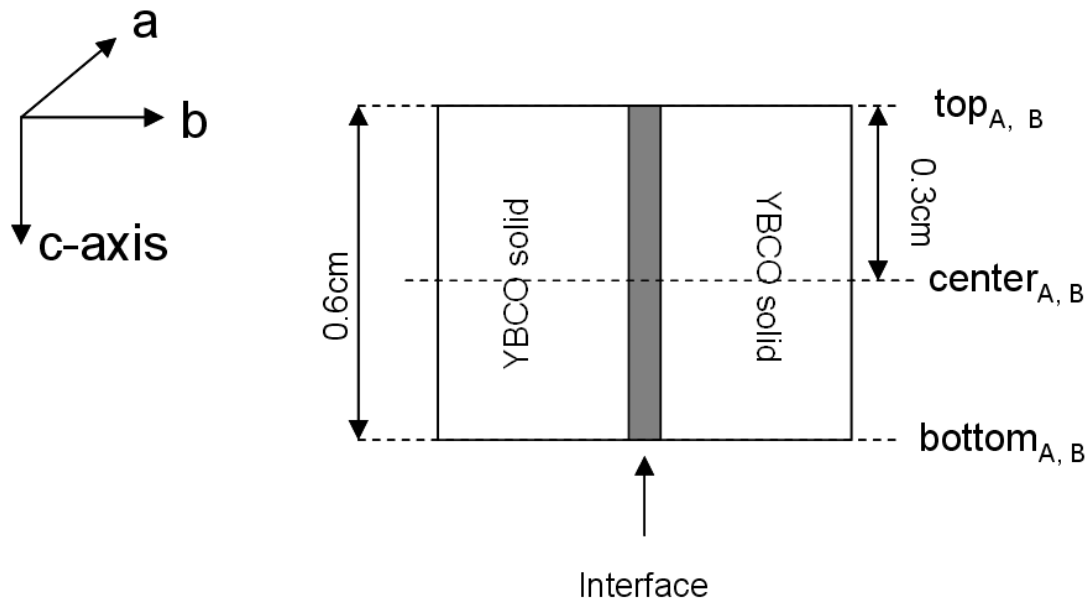


Figure 6.43: Schematic drawing of YBCO/Ag/YBCO joints cut into two slices parallel to the ab planes.

from the top face towards the bottom face the porosity is more persistent. This difference arises from the primary microstructure of the YBCO samples used for the welding process which were grown by Top Seeding method.

Moreover, note the difference in microstructure around the interface. When the top face is analyzed, the good quality joint represents $\approx 38\%$ from the total length of the junction, as determined from microstructural analysis. As shown in the figure, Ag particles together with some $BaCuO_2$ -CuO phase are captured while moving away from the center of the junction. At the edges of the junction, these agglomerates are extended up to $500\mu\text{m}$ inside the YBCO matrix whereas in the rest of the material only up to $125\mu\text{m}$. A silver free region is observed at the central part of the junction and the crystallization is completed at this part of the sample.

When the center face is investigated, the junction displays a discontinuity. The Ag precipitates and the $BaCuO_2 - CuO$ phases have been captured all along

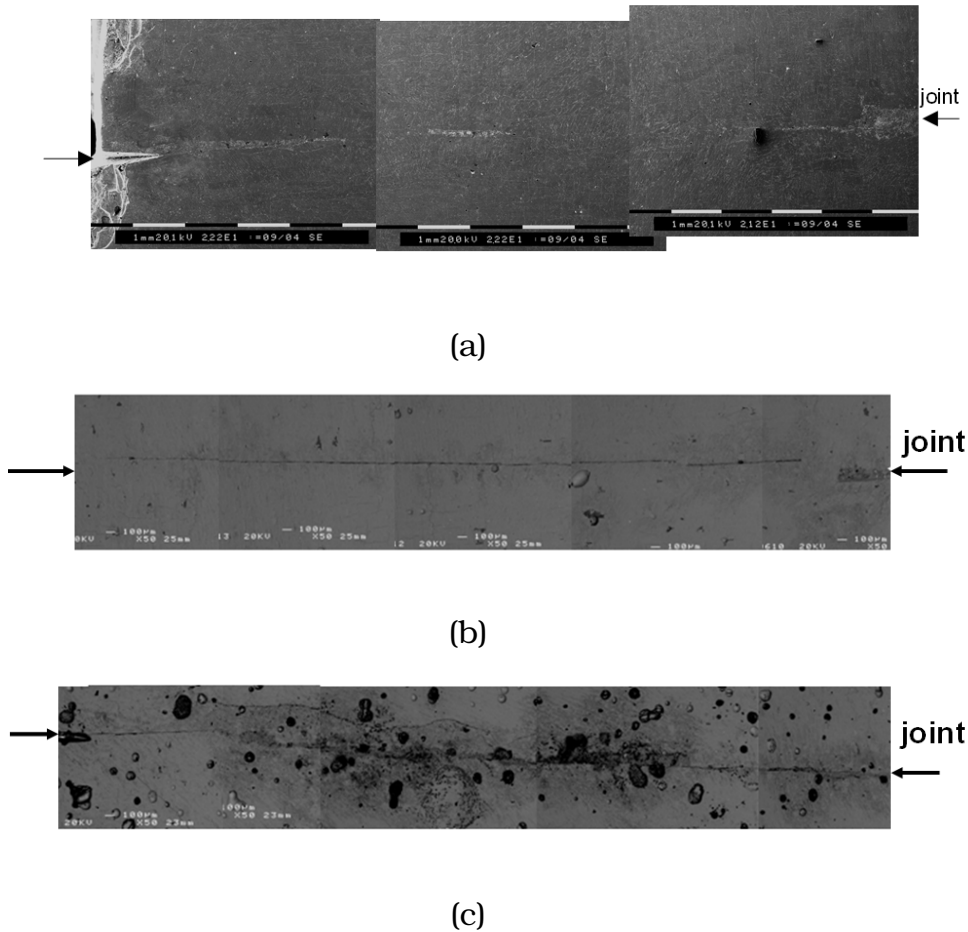


Figure 6.44: Microstructure of an ab plane of a YBCO/Ag/YBCO joint obtained by using a cooling rate of $r=6^{\circ}\text{C}/\text{h}$. a) top face; b) center face; c) bottom face

the interface but at the edges there are extended up to $200\mu\text{m}$ inside the YBCO matrix. In figure 6.45 the junction is observed at a higher magnification. EDX analysis have been done inside the junction, as it is indicated in figure 6.46. According to EDX data (see figure 6.46a and b) this region contains predominantly Ag, and some amount of Ba and Cu which would be consistent with a solidified $\text{BaCuO}_2\text{-CuO}$ liquid.

In the case of bottom face (*bottom_A*) many voids and non-superconducting phases were observed at the interface (see figure 6.44c). There is no continuity through the joint and the porosity is extended all along the joint. The YBCO

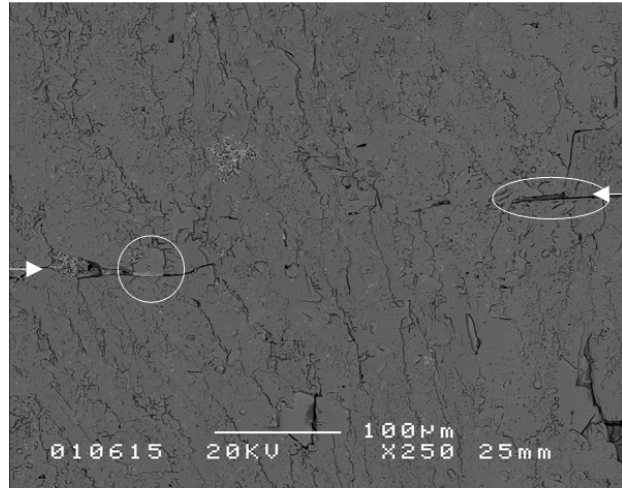


Figure 6.45: Detail of the YBCO/Ag/YBCO interface when the joint is grown by using a cooling rate of $r=6^{\circ}\text{C/h}$; the interface is indicated by white arrows.

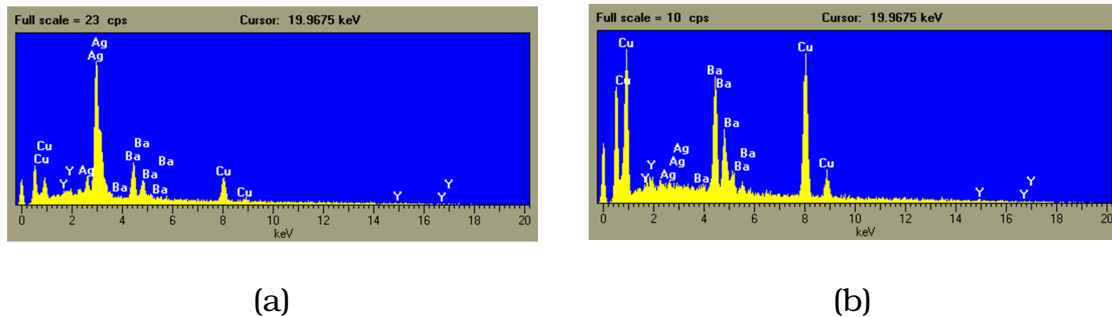


Figure 6.46: EDX analysis inside an YBCO/Ag/YBCO interface corresponding to the sample A obtained by using a cooling rate of $r=6^{\circ}\text{C/h}$. a) Ag precipitates and b) BaCuO_2 phase.

matrix is even more porous than in the other cases. This porosity is a characteristic of the primary microstructure of the YBCO domains, being the result of the processing method of the YBCO monoliths.

In figures 6.47(a-c) are represented the top, center and bottom faces, respectively, corresponding to the sample B. As in the previous case, note that these faces present different microstructures while moving away from the top towards the bottom face. For all the faces, the Ag particles and BaCuO_2 -CuO phases were trapped at the edge of the sample. The quality of the center face is im-

proved when compared with the center face of the sample A. This is a result of the cooling rate; the sample A being grown at a cooling rate higher than sample B. For sample B, the joint length free of any non-superconducting phases represents $\approx 42\%$ from its total length. The remaining 58% displays a porous, zone where Ag particles and $BaCuO_2$ -CuO phases are captured during the welding process.

Summarizing, in order to image the 3D Ag diffusion phenomenon into the YBCO matrix, we have analyzed different ab-plane faces of the joints along the c-axis. The samples studied showed different quality degrees and it has become clear that a full consideration of the defects distribution appearing during the welding process is required. Indeed, the different ab faces investigated across the joint ceramic samples show different microstructures. Basically, it was found that the top face exhibits the best quality from the microstructural point of view. The inner part of the top face junction seems to crystallize first and then the Ag-rich liquid together with $BaCuO_2$ -CuO liquid phase are pushed towards the edge of the sample. On the other hand, the center face junction usually shows porosity which can be extended along the junction depending on the cooling rate used. Some Ag and $BaCuO_2$ -CuO phases have been detected inside the porous region. When the cooling rate is too high, the discontinuity can be extended all along the junction length, whereas when the cooling rate is lower the interior part of the junction has crystallized while the edges present some inhomogeneities associated with Ag-rich liquid and $BaCuO_2$ -CuO phase. On the contrary, for both samples, the bottom face exhibits inhomogeneities all along the junction and have a lower superconducting quality.

This difference between the top and bottom faces of the junction could be a consequence of the microstructure of the starting YBCO samples. In Chapter 4, when the top seeding process used to determine the starting YBCO material has been explained, it has been mentioned that the bottom part of the initial big monoliths should be eliminated because of the high porosity and Y211 phases

found in the matrix. Thus, before the inserting of Ag foil between the YBCO single domains for the welding process, the porous and inhomogeneous part of the sample has been cut. Even after the elimination of 0.8cm from the thickness of the YBCO sample, some porosity and inhomogeneity still remained at the bottom face.

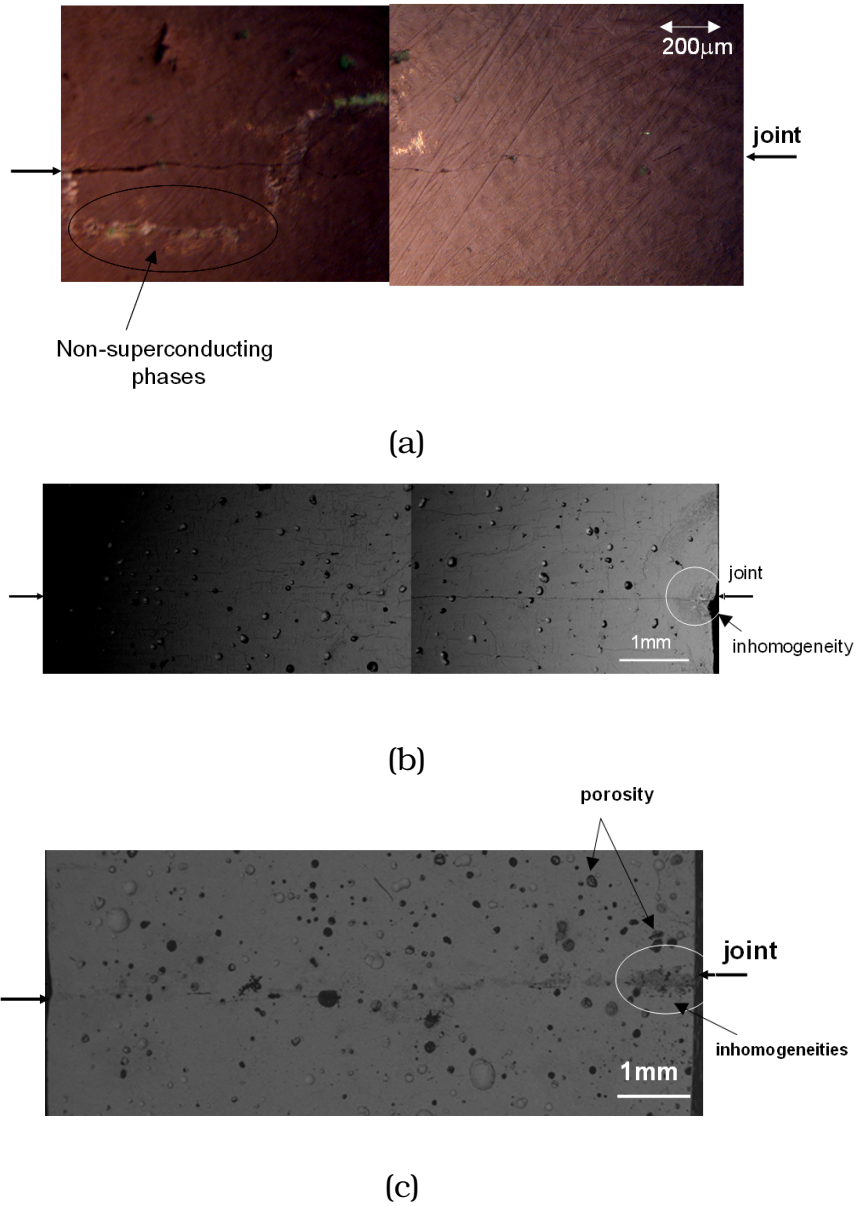


Figure 6.47: Microstructure of an ab plane of a YBCO/Ag/YBCO joint obtained by using a cooling rate of $r=3^{\circ}\text{C}/\text{h}$. a) top face (optical micrograph corresponding to a section of $0.24 \times 0.1 \text{ cm}^2$); b) center face (SEM micrograph corresponding to all the length of the joint); c) bottom face (SEM micrograph corresponding to all the length of the joint). The joint is indicated by arrows.

6.3 Conclusions of the Chapter

A deep study of the influence of different parameters on the microstructure of the final joints generated using a YBCO/Ag/YBCO architecture has been performed in order to understand the role of the Ag diffusion and to optimize the welding process. Different microscopic techniques have been employed such as: optical microscopy and SEM. Moreover, chemical analysis using WDS and EDX have been done at the junction and inside the YBCO matrix to observe the Ag diffusion process.

According to the results presented in this Chapter, the Ag diffusion process in the investigated system is very complex. After a sequential investigation of the role played by different parameters, we can conclude that each parameter influences in one way or another the final quality of the joints. Two kind of thermal processes have been used in this study: quench experiments and slow cooling experiments. In the quench experiments, parameters such as: melting time (t_{melt}), Ag thickness (g_{Ag}) and weld configuration have been investigated and optimized for the obtention of a high quality joint. On the other hand, parameters such: cooling rate (r), processing temperature (T_{max}) and temperature window (ΔT) have been analyzed by means of slow cooling experiments.

It has been shown that a (100)/(100) weld configuration, a melting time of $t_{melt}=3$ hours, a processing temperature of $T_{max}=992^{\circ}\text{C}$, a cooling rate of 0.6°C/h and a window temperature of $\Delta T=28^{\circ}\text{C}-33^{\circ}\text{C}$ are optimum to achieve an optimized microstructure, when Ag foils with a thickness of $10\ \mu\text{m}$ are used.

Some of the samples studied in this PhD thesis have been used in order to observe the homogeneity in the microstructure along the ab plane while moving away from their top face towards the bottom face. It has been observed that the cooling rate plays an important role on the Ag diffusion into YBCO matrix. By studying this parameter we have noticed that the welding process is based on the Ag pushing phenomena [51].

A 2D Ag diffusion model has been proposed in Section 6.3 which establishes

that Ag rich liquid is pushed away from the inner part of the sample towards its edges along the YBCO growth interface. The crystallization is first completed in the inner part where the Ag-rich liquid was completely expelled. It turns out then to use a cooling rate slow enough to expel all the Ag from the interface and high enough to maintain the size of Ag droplets below the critical size. When the cooling rate was $r=3^{\circ}\text{C}/\text{h}$ the homogeneity in ab-plane faces along c-axis is quite homogeneous, exhibiting a similar microstructure. Some difference in the porosity which exhibit each face can be seen. But this difference is a characteristic of the YBCO samples obtained by Top Seeding process.

